Journal of Applied Polymer Science

Simultaneous Polypropylene Functionalization and Nanoclay Dispersion in PP/Clay Nanocomposites using Ultrasound

Juan G. Martínez-Colunga,[1] Saul Sánchez-Valdés,[1] L. F. Ramos-deValle,[1] Libertad Muñoz-Jiménez,[1] Eduardo Ramírez-Vargas,[1] Maria Cristina. Ibarra-Alonso,[1] Tomas Lozano-Ramirez,[2] Pierre G. Lafleur[3]

[1]Centro de Investigación en Química Aplicada, Blvd. Enrique Reyna No.140 C. P. 25253 Saltillo Coahuila, México

[2]Instituto Tecnológico de Cd. Madero, Juventino Rosas y Jesus Urueta, C.P. 89440 Cd. Madero, Tamaulipas, México

[3]Ecole Polytechnique de Montreal, Chemical Engineering Department P.O Box 6079, Stn Centre-Ville, Montreal, Quebec H3C 3A7, Canada

Correspondence to: J. G. Martínez-Colunga (E-mail: guillermo.martinez@ciqa.edu.mx)

ABSTRACT: Polypropylene nanocomposite materials were prepared with 5 and 10 wt % cloisite C20A clay, jointly with 0.6 and 1.2 wt % of maleic anhydride (MA) for the simultaneous polymer functionalization and clay dispersion in a twin screw extruder assisted with ultrasonic irradiation, using different sonication intensities (231, 347, and 462 W, which correspond to 30%, 45%, and 60% of the maximum instrument intensity, "770 W") all in a single-step operation. The MA polymer functionalization was followed by FTIR spectroscopy and determined by titration. The increase in modulus of the obtained PP/Clay nanocomposites was attributed to the greater dispersion level, presumably achieved becuase of the joint application of the PP–Clay compatibilization with MA and the sonication during processing in a twin screw extruder. The greater level of clay dispersion was verified by the displacement of the XRD diffraction peak to lower angles, indicating an intercalated-exfoliated structure that was corroborated by STEM. © 2014 Wiley Periodicals, Inc. J. Appl. Polym. Sci. **2014**, *131*, 40631.

KEYWORDS: composites; extrusion; grafting; nanostructured polymers; polyolefins

Received 6 November 2013; accepted 21 February 2014

DOI: 10.1002/app.40631

INTRODUCTION

The addition of nanofillers into a polymer matrix has given rise to a new class of materials, generally referred to as nanocomposites, with a notable improvement in mechanical properties mainly in modulus, heat resistance, and gas and solvent barrier, among others.[1] The effect of nanoclays as nanofillers, on the properties of different polyoleofins such as polypropylene has been intensely studied.[2] The interfacial interactions between the polyolefin chains and the clay layers play an important role because the final structure of the nanocomposite depends on these interactions, which play an important role in achieving an exfoliated or intercalated structure.[3] The exfoliation of the normally aggregated-stacked structures of montmorillonite (tactoids) during polymer processing, is highly difficult.

Becuase of their relatively large size, and their incompatibility towards polyolefines, these tactoids induce local tensions when the polymer-clay nanocomposites are deformed, and as a result the elongation at break and the impact strength become very low. Therefore, compatibilization and dispersive mixing are of the utmost importance in order to achieve the best mechanical properties in the nanocomposite.[4] Maleic anhydride (MA)-modified polypropylene is commonly used as compatibilizing agent.[5–8] This chemical modification adds polar groups to polyolefins, resulting in reactive centers that increase polymer–filler or polymer–polymer interfacial interaction.[9,10] The selection of the monomer to be grafted into the polyolefin, which will generate the compatibilizing agent, should be done considering that it must have unsaturations, polar groups and be stable at the functionalization reaction temperatures. The most used monomers for the PP modification are acrylic acid, MA, Zigler-Natta catalysts, borane derivatives,[11] esters, and carboxylic acids,[12] although the most reported moiety is the MA[13–19]. The grafting of MA to polyolefins is usually performed in the extruder, using peroxide as an initiator.[20–36] On the other hand, the modification of polypropylene with MA, via extrusion with the assistance of ultrasonic irradiation, has also been reported.[37]

The presence of fillers in the PP matrix provides a substantial increase in the modulus and thermal resistance, as well as on

Table I. Ultrasound Intensities, Nanoclay, and MA Contents Studied

Nanoclay contents (%)	MA contents (%)	Ultrasound intensities (W)
		0
5	0.6	231
10	1.2	347
		462

the melt viscosity of the nanocomposite. Additionally, the addition of fillers also increase the dimensional stability of the nanocomposite.[12,38]

It has been reported, on the other hand, that exfoliation or dispersive mixing can be boosted by the assistance of ultrasound.[4] Of particular interest in this study, is the double effect of sonication; the tendency to generate macro-radicals along the polymer chains, which would eventually be the points for the MA functionalization and the exfoliation or dispersive mixing of the nanoclay into the polymer matrix.

EXPERIMENTAL

Materials

Materials used were: isotactic Polypropylene (iPP) VALTEC HP423M, with MFI of 4 g/10 min and density of 0.9 g/cm^3, from INDELPRO, Mexico; 95% pure MA and KOH powder, from Aldrich, USA; reagent grade xylene, acetone, and ethanol from by JT Baker, USA, which were used as received; and montmorillonite nanoclay Cloisite 20A, from Southern Clay Products, USA.

Preparation of Nanocomposites

Nanocomposites were prepared in a W & P twin screw extruder ZSK −30 at 160°C in the feeding section and 210°C in the other extruder sections, including the die head and die, running at 75 rpm. A MISONIX ultrasound equipment with a working frequency of 20 kHz and maximum intensity output of 770 W was placed in the die head and various intensities were assessed. Detailed information of the prepared samples is presented in Table I. Previously dried in a vacuum oven at 60°C for 4 hours, the nanoclay was added at concentrations of 5 and 10 wt %. After extrusion and pelletizing, 13 × 13 × 2 mm laminates were obtained via compression molding using a PHI press, at 200°C and 12 MPa.

The PPgMA levels used were based on a previous study on our labs of PP/Clay/PPgMA nanocomposites[39]. In this new study, we maintained the ratio of PPgMA:Clay at 3:1. In this sense, for 5 wt % clay, we added 15 wt % of PPgMA (with 1 wt % MA). Additionally, in accordance to Peng et al.[40] and Yaqin et al.,[41] and assuming similar efficiencies, we tried ultrasound intensities of 231, 347, and 462 W.

Characterization

The amount of MA grafted onto the iPP was determined by FTIR spectroscopy and quantified by titration by the dilution of the nanocomposite samples in hot xylene at 120°C, followed by precipitation with acetone and finally washing the precipitate with acetone for up to 10 times to remove the unreacted MA.

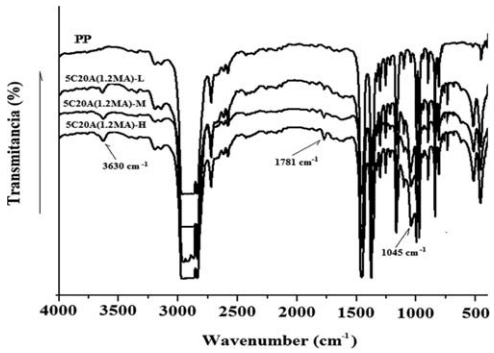

Figure 1. FTIR spectra of (a) pure PP and (b) PP nanocomposites with 5 wt % C20A and 1.2 wt % MA with low (L), medium (M), and high (H) intensity ultrasound treatment.

The exfoliation and dispersion was determined by XRD and verified by STEM. Tensile strength and flexural modulus were determined in accordance to the ASTM D638 and D790, respectively. The thermal properties and thermal stability were determined by differential scanning calorimetry (DSC) and thermogravimetric analysis (TGA), respectively.

RESULTS AND DISCUSSION

Infrared Spectroscopy

FTIR spectra of pure iPP and iPP/clay nanocomposites with 5 wt % C20A and 1.2 wt % MA, processed with ultrasonic irradiation are shown in Figure 1. The characteristic bands of pure iPP such as those corresponding to CH_3, CH_2, and CH groups at 1380, 1460, and 1160 cm^{-1} respectively, can be seen in this figure.

In the nanocomposite samples a band at 3630 cm^{-1} related to the OH of the Al-OH and Si-OH and a band at 1045 cm^{-1} attributed to the Si-O group of the clay can also be seen. The MA characteristic band is observed at 1781 cm^{-1} which increases with the ultrasonic irradiation intensity. This indicates that the MA grafting into PP is stimulated by the application of ultrasound.

The MA grafting degree into PP nanocomposites was determined by titration and is shown in Figure 2. The effect of the

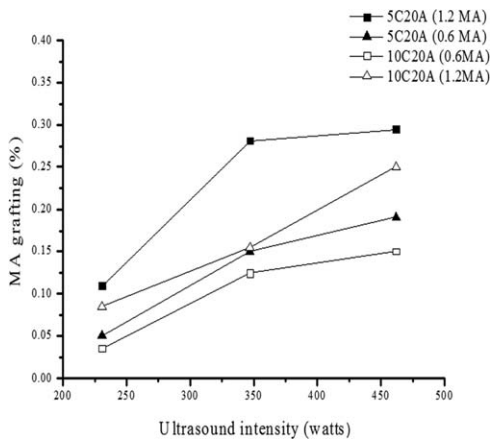

Figure 2. Effect of MA grafting with ultrasound intensity at various Clay and MA contents.

Table II. MA Grafting Efficiency[a] of the PP Nanocomposites as a Function of the Initial MA Content (0.6 and 1.2 wt %) and the Applied Ultrasound Intensity

	5 wt % Clay		10 wt % Clay	
Ultrasound intensity [W]	0.6 wt % MA	1.2 wt % MA	0.6 wt % MA	1.2 wt % MA
231	8.7	8.6	6.6	6.5
347	25.0	22.2	20.7	14.6
462	31.8	24.5	25.0	20.8

[a] Graft Eff. = (wt % attained -from Figure 2) × 100 / (initial MA wt % −*0.6 or 1.2* wt %)

initial MA content (0.6% and 1.2%) can be seen in this figure. The greater the initial MA content, the greater the grafting degree. It can also be seen that the higher the applied ultrasonic energy, the greater the grafting degree attained. This indicates that the higher ultrasonic energy can promote the formation of more PP macroradicales that can support the grafting reaction with MA. This has been previously reported;[40,42] although there are reports of negative effects of ultrasound on MA grafting into PP in the melt.[41]

The grafting efficiency, on the other hand, decreased as the MA content increased, as observed in Table II. In addition, the greater the ultrasound intensity, the greater the difference in efficiency between the two different initial MA content studied. This decrease in the MA grafting efficiency has been reported by other authors[40,41] and is attributed to several factors such as; MA grafting saturation, limited solubility of MA into the PP melt, and that under the selected reaction conditions, the MA radicals may undergo dismutation reactions, (that is, one lateral undesired reaction plus the desired grafting reaction).[41] In the present study, any or all of the above mentioned factors may be involved. But another factor that may play a role is the lubricating effect of the excess MA, which reduces the mixing shear stress, reducing so the grafting efficiency. This behavior is more extensively discussed below. Another factor could be the MA interaction with the clay, which may hinder its diffusion through the PP macro-radicals. As observed in Figure 2, the relationship of the applied ultrasound intensity with the MA grafting concentration is consistent with that reported by Zhang[42] and Peng.[40]

It is also observed that the clay content adversely affects the MA grafting level. This behavior may be attributed to several factors, one would be the lower polymer content when the clay content is increased, and another could be the difficulty for MA diffusion because of the interactions between MA and the polar groups in the clay surface.

X-ray Diffraction

The extent of clay exfoliation in the nanocomposites was assessed by XRD as shown in Figures 3 and 4, for nanocomposites with 5 and 10 wt % clay, respectively; for 0.6 and 1.2 wt % MA, without and with the ultrasonic irradiation. Additionally,

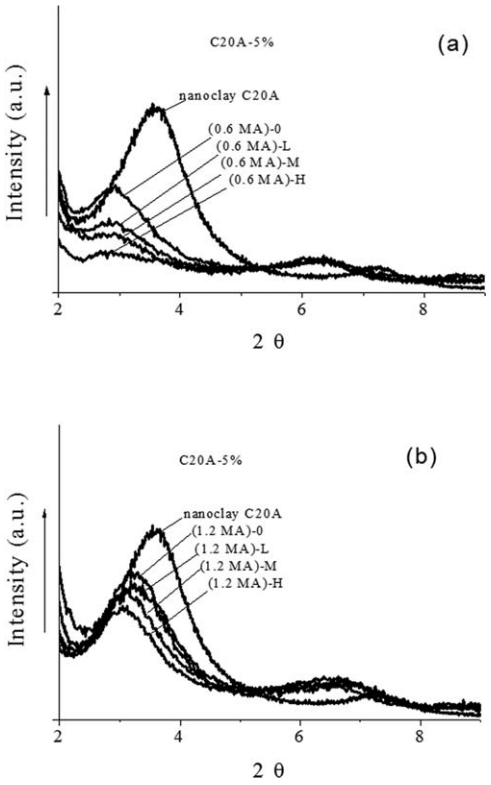

Figure 3. XRD patterns of C20A clay and PP/Clay nanocomposites with 5 wt % clay at various ultrasoundintensity treatments, with: (a) 0.6 wt % MA and (b) 1.2 wt %MA.

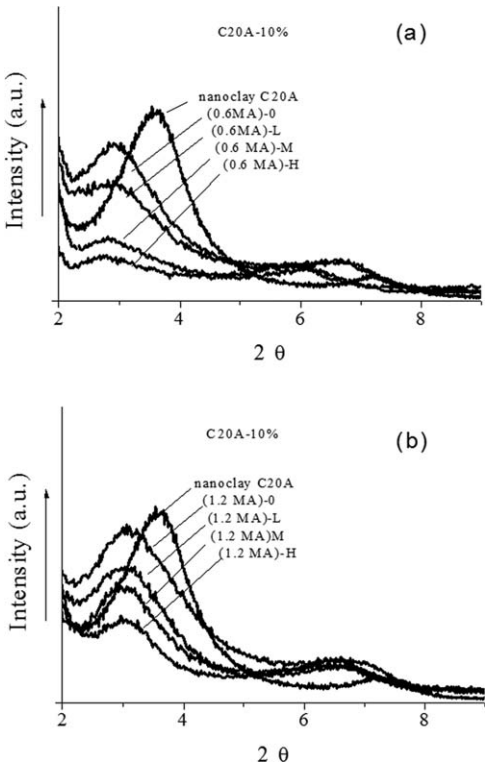

Figure 4. XRD patterns of C20A clay and PP/Clay nanocomposites with 10 wt % clay at various ultrasound intensity treatments, with: (a) 0.6 wt % MA and (b) 1.2 wt % MA.

Table III. Effect of Ultrasound Intensity, Clay Content, and MA Initial Concentration on the Diffraction Angles and Intergallery Spacings of C20A Nanoclay, in PP/Clay Nanocomposites

5 wt % C20A clay			10 wt % C20A clay		
Nanocomposite	2θ	d_{001} (Å)	Nanocomposite	2θ	d_{001} (Å)
C20A	3.5	25.1	C20A	3.5	25.1
1.2MA-0	3.2	28.3	1.2MA-0	3.2	27.6
1.2MA-L	3.0	29.0	1.2MA-L	3.2	27.9
1.2MA-M	3.1	28.8	1.2MA-M	3.1	28.5
1.2MA-H	3.1	28.8	1.2MA-H	3.1	28.3
0.6MA-0	2.9	30.2	0.6MA-0	3.1	28.7
0.6MA-L	2.9	30.4	0.6MA-L	3.1	28.7
0.6MA-M	2.8	31.1	0.6MA-M	3.1	28.8
0.6MA-H	2.8	31.5	0.6MA-H	2.9	30.6

Table III shows the diffraction angles and interlayer spacing (d_{001}) for all the analyzed nanocomposites.

In both cases, the nanocomposites without the ultrasound irradiation exhibited higher peaks and a certain displacement to lower angles, which was taken as indicative of a certain degree of clay intercalation. The ultrasound-treated nanocomposites, on the other hand, showed smaller peaks and more significant displacements towards smaller diffraction angles.

The greatest peak displacement and smallest peak intensity was observed in the 0.6 wt % MA nanocomposites when applying the high intensity ultrasound irradiation.

Nanocomposites with 10 wt % clay presented broader diffraction peaks, emphasizing the greater difficulty for clay exfoliation, as the clay concentration increases. This behavior was also observed by Xidas et. al.[43] using different I28E clay concentrations (3, 6, and 10 wt %) in a rubber-epoxy nanocomposite (I28E clay from Nanocor Company).

The obtained clay peaks displacements are significant as can be seen in Figure 4, but is even more significant the reduction in the diffraction peak intensity for nanocomposites treated with ultrasound as compared to those without treatment. This indicates that ultrasound application may reduce the amount of ordered clay structures and as a consequence, the ultrasound energy also has an effect on the exfoliation-intercalation structure.

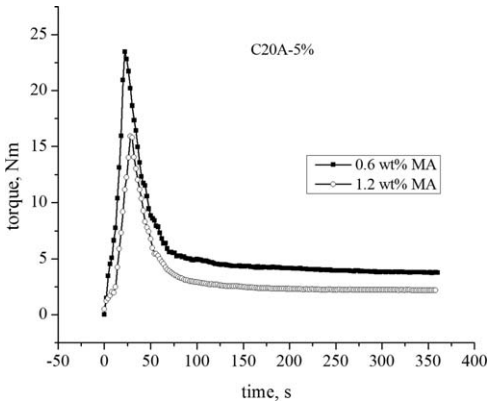

Figure 5. Mixing torque of PP-clay nanocomposites with two different MA contents.

According to Vaia et al.,[44] an XRD diffractogram where no shift signals are observed will correspond to a completely exfoliated/delaminated clay. Diffractograms where a peak displacement is observed, on the other hand, indicate that the clay individual laminates remain stacked as tactoids. This explains the diffraction patterns of nanocomposites with 5 wt % clay and 0.6 wt % MA with high ultrasound intensity [Figure 3(a)] which clearly show a small peak of low intensity; indicating the co-existance of exfoliated and intercalated structures.

Data summarized in Table III show the positive effect of ultrasonic irradiation in the clay exfoliation-intercalation. Increasing the ultrasound intensity, results in a decrease in the clay diffraction peak and a small but noticeable displacement of this peck towards smaller angles. This effect is attributed to the high ultrasound energy that can destroy the clay platelets order, decrease the tactoids size and favor the penetration of polymer chains through the clay galleries. This will result in an intercalation and exfoliation structure as shown in the micrographs of Figure 6.

The negative effect of increasing the MA content, on the clay exfoliation, Figure 4(B), was attributed, as mentioned above, to the lubricating effect of the increased MA content.

None of the ultrasound treated nanocomposites showed a complete disappearance of the clay diffraction peak, which leads to the assumption that some clay tactoids still exist. From Figures 3 and 4, and Table III, it was noticed that samples with 0.6 wt % MA, as compared to those with 1.2 wt %, showed the greater peak displacements and smaller peak intensities. In order to determine the cause of this behavior, two PP nanocomposites with 5 wt % Clay, with 0.6 and with 1.2 wt % MA were prepared in a Brabender Torque Rheometer mixing chamber at 60 rpm and 180°C. Figure 5 shows the mixing torque along the 6 minutes of mixing, where it can clearly be observed that the lower MA content required a higher mixing torque. This indicates that an increase in the MA content appears to act as a

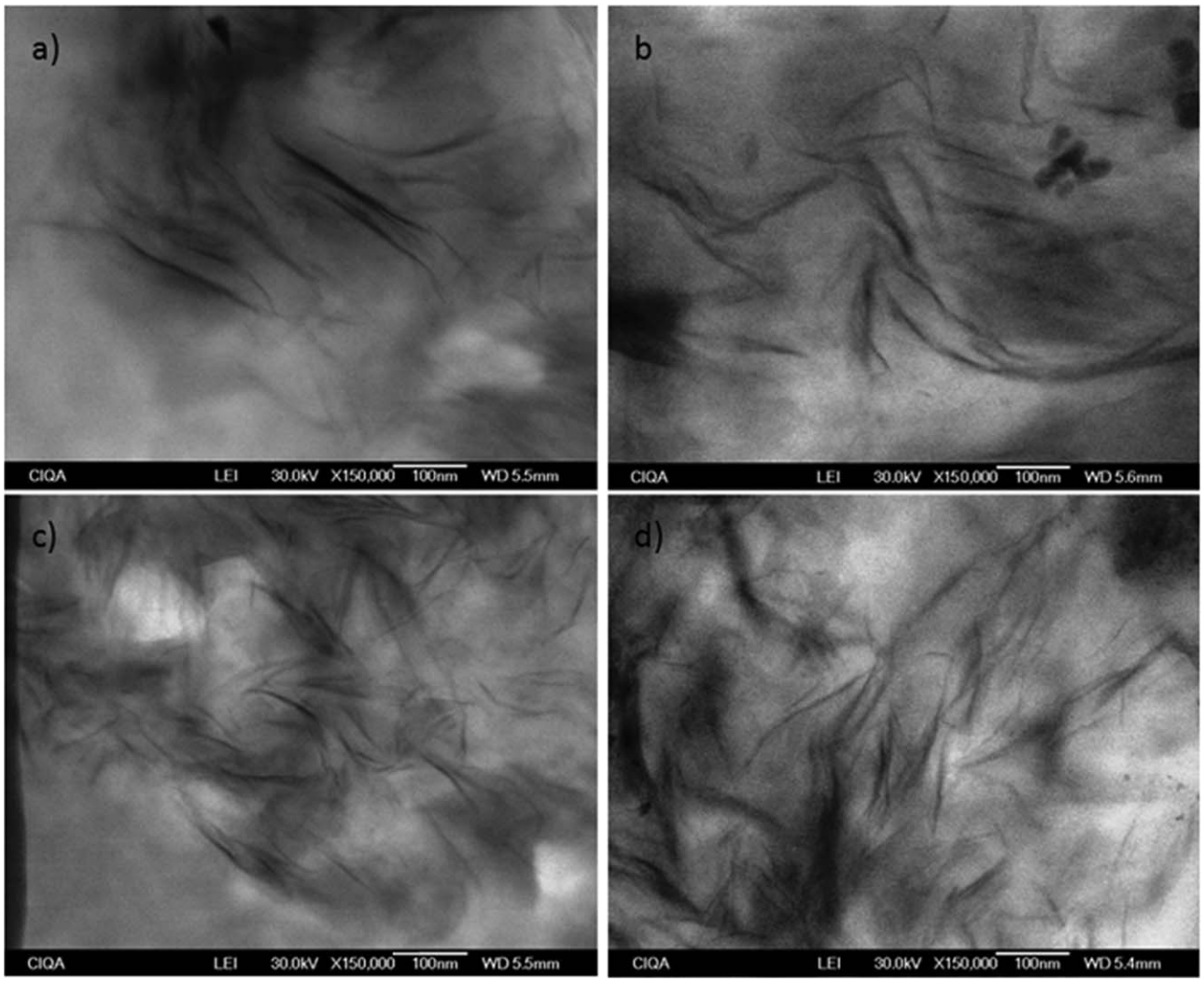

Figure 6. STEM micrographs of nanocomposites with 5 wt % clay and 0.6 wt % MA: (a) without ultrasound, (b) with 231 W of ultrasound, (c) with 462 W of ultrasound, and (d) with 10 wt % clay and 0.6 wt % MA, with 231 W of ultrasound.

lubricant, reducing the shear stress transmitted into the system, and diminishing so the level of dispersive mixing attained; even with the application of ultrasound and the *in situ* generation of the compatibilizing agent.

It is well known that exfoliation of nanoclay in a polyolefin/clay nanocomposite occurs mainly becuase of the shear exerted on the nanocomposite during mixing;[45] but it is also known that this exfoliation is facilitated by the organo-modification of the clay through the insertion of large molecules, which; (a) expands the clay inter-gallery spacing and (b)- decreases the polarity of the clay. This expansion will open the way for the the insertion of the non-polar polyolefin chains promoting the exfoliation.

According to the XRD results, the particular case of nanocomposites with 5 wt % clay and 0.6 wt % MA showed a high degree of exfoliation-intercalation. This was attributed to the simultaneous occurrence of the MA grafting into PP and the destruction of clay tactoids, both reinforced by the ultrasound application.

Electronic Microscopy

Figure 6 shows STEM images of nanocomposite with 5 wt % clay, 0.6 wt % MA without and with the ultrasound treatment at various intensities. Nanocomposites without ultrasound treatment present a large number of clay aggregates or tactoids [Figure 6(a)] with certain regions with intercalated structures. On the other hand, micrographs of nanocomposites treated with ultrasound showed only a few tactoids and noticeable greater clay exfoliation [Figure 6(b,c)], with the higher exfoliation level occurring at the higher ultrasound intensities [Figure 6(c)].

Application of ultrasound significantly reduces the size of tactoids with a clear tendency towards complete exfoliation, though some small tactoids can still be observed. This corroborates the XRD analysis results. The micrograph of the nanocomposite with 10 wt % clay and 0.6 wt % MA is shown in Figure 6(d), where the structure appears more intercalated than exfoliated, which is attributed to the clay content having exceeded the saturation concentration.

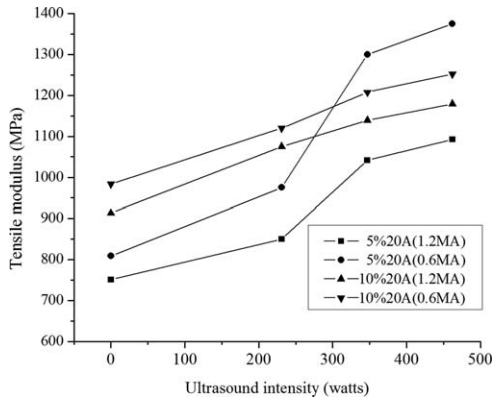

Figure 7. Effect of ultrasound intensity on the tensile modulus of PP/Clay nanocomposites.

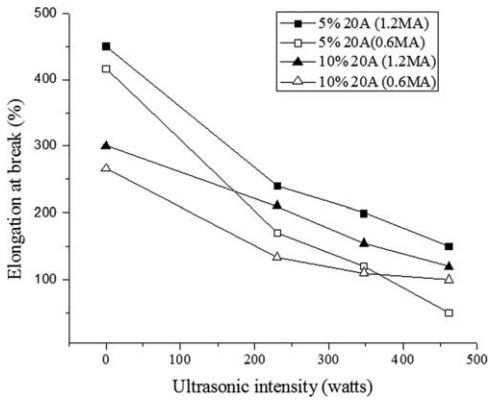

Figure 8. Effect of ultrasound intensity on elongation at break of PP/Clay nanocomposites.

This confirms that although the XRD results indicate a slight increase in the inter-gallery spacing at high clay content, the attraction forces between clay platelets predominate over those forcing the penetration of the polymer chains through the clay galleries, resulting in a lesser degree of intercalation-exfoliation.

Mechanical Properties

With respect to the mechanical properties of nanostructured composites, these are determined by the polymer matrix properties, by the microstructure and morphology of the composite and by the nanoparticles concentration, distribution, dispersion, and orientation, as well as by the nature of the polymer–nanoparticles interactions. Lapshin et al.[46] reported that PP/Clay nanocomposites mechanical properties are significantly increased in ultrasound-assisted extruded products. Swain et al.[47] reported that the addition of 5–10 wt % nano-fillers, significantly increases their modulus but this property slightly decreases when increasing the amplitude of the applied ultrasound. These reports indicate that the effect of ultrasound on the nanocomposite mechanical properties is still not well understood.

On this respect, Figure 7 shows the effect of ultrasound intensity on the tensile modulus, of PP/Clay nanocomposites with different Clay and MA contents. First, it was observed that in all cases, the tensile modulus increased with the applied ultrasound intensity. Second, it was observed that an increase in MA content produced a decrease in modulus, which is attributed to the lubricating effect of the MA. Third, the effect of clay content is somewhat different.

Looking at the nanocomposites prepared without an ultrasound treatment (*ultrasound intensity equal to zero*), it is observed that for the same MA content, the tensile modulus increases with the clay content (*as commonly observed when increasing the filler content*), but decreases with increasing the MA content (*becuase of the already mentioned lubricating effect of the MA*). But as the ultrasound intensity increases from low to medium to high, the tensile modulus of the nanocomposites with the lower clay content (5 wt %) tends to show much greater increments than that shown by the nanocomposites with the higher clay content (10 wt %). It is clearly seen that nanocomposites with 5% clay and 0.6 wt % MA showed the highest increase, eventually attaining the highest modulus. It can be assumed that the 10 wt % clay concentration has surpassed the saturation point. This is because; as the ultrasound heightens the exfoliation/comminution of the clay tactoids, this generates much more clay particles of smaller and smaller sizes. And as the particle size decreases, the number of individual particles increases and the saturation point is achieved at lower and lower concentrations. These results coincide with the XRD and STEM results, in which nanocomposites with 5 wt % clay and 0.6 wt % MA showed the most exfoliation-intercalation.

The increase in modulus with increasing ultrasound intensity is a clear indicative of a greater clay exfoliation or comminution with the ultrasound[46,47] which besides promotes the grafting of MA onto the PP chains

Elongation, as shown in Figure 8, presents a behavior somewhat contrary to that observed with modulus. In all cases, the elongation decreases with the applied ultrasound intensity. Also, when no ultrasound treatment is applied, the elongation decreases with the clay content. Finally, an increase in the MA content produces a slight increase in elongation.

It can be seen that the lowest elongation is presented by the nanocomposite with 5 wt % clay and 0.6 wt % MA. This lower elongation was attributed to the lower molecular chain mobility, which becuase of the greater level of exfoliation, results in a much greater filler surface area in contact with the polymer chains, hindering thus the chain mobility; resulting so in lower elongation.

TGA Analysis

With respect to the thermogravimetric analysis, Figure 9 shows the weight loss with temperature of PP/Clay nanocomposites with 5 wt % clay, at 0.6 and 1.2 wt % MA concentrations and treated with high and low ultrasound intensities.

First, it is clearly seen that all nanocomposites present a higher decomposition temperature than the pure PP, and second, the decomposition temperature of all nanocomposites is practically the same. Nanocomposite with 0.6 MA and high intensity ultrasound treatment, presented a slightly higher decomposition temperature. The decomposition temperature of the 10 wt %

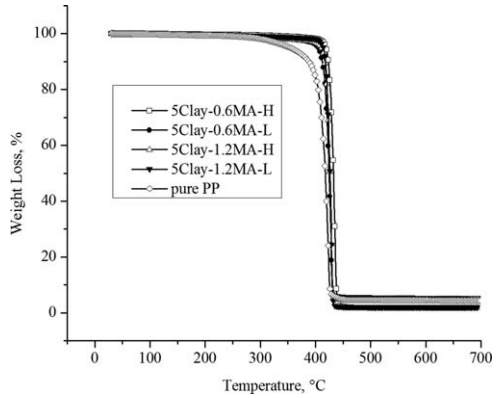

Figure 9. TGA thermograms of the nanocomposites with 5 wt % clay, 0.6 and 1.2 wt % MA, and high and low ultrasound intensities.

clay nanocomposites, not shown here, presented almost identical decomposition temperatures.

The ultrasound intensity showed a minor effect on the thermal stability. Samples treated with high ultrasound intensity showed a slightly higher thermal stability than those prepared with low intensity, particularly those with the smaller amount of MA.

This behavior is related with the clay dispersion/comminution. It has been reported that a greater degree of intercalation and exfoliation promotes a greater barrier to the diffusion of gases such as oxygen and combustion gases.[47] With these results it can be say that ultrasound induces higher material thermal stability.

CONCLUSIONS

The joint application of ultrasound irradiation and MA addition, during the preparation of PP/Clay nanocomposites in a twin screw extruder showed to have a very significant effect on the simultaneous grafting of MA onto the PP chains and in the exfoliation/dispersion of the clay.

It was observed that the greater the initial MA content and the higher the applied ultrasonic energy, the greater the grafting degree attained.

The grafting efficiency, on the other hand, decreased as the MA content increased.

The greatest peak displacement and smallest peak intensity, that is, the highest level of exfoliation/dispersion, was observed in the 5 wt % clay and 0.6 wt % MA nanocomposites, when applying the high intensity ultrasound irradiation.

In all cases, the tensile modulus increased with the applied ultrasound intensity, whereas an increase in the MA content produced a decrease in modulus. Elongation presented a behavior somewhat contrary to that observed with modulus. In all cases, the elongation decreases with the applied ultrasound intensity.

ACKNOWLEDGMENTS

Two of the authors, L. Muñoz-Jiménez and M. C. Ibarra-Alonso, wish to thank Conacyt for a scholarship to carry out their MSc studies. Also, the authors gratefully acknowledge the financial support of CONACyT through projects: CB-104865 and CB-84424. The authors would also like to thank M. C. Gonzalez-Cantu, J. Zamora-Rodriguez, M. Lozano-Estrada, M. L. Lopez-Quintanilla, G. Mendez-Padilla, J. Rodriguez-Velazquez, J. F. Zendejo-Rodriguez, H. Jimenez Zúñiga, A. Ordáz Quintero Araceli-Noxpanco, Alejandro-Espinoza, Marcelina-Sanchez, Fabian-Chavez, M Lourdes-Guillen, Jose Lopez-Rivera, Silvia-Torres and Miriam-Lozano for their technical assistance.

REFERENCES

1. Wu, J. -Y.; Wu, T. -M.; Chen, W. -Y.; Tsai, S. -J.; Kuo, W. -F.; Chang, G. Y. *J. Polym. Sci. B Polym. Phys.* **2005**, *43*, 3242.
2. Yano, K.; Usuki, A.; Okada, A.; Kurauchi, T.; Kamigaito, O. *J. Polym. Sci. A Polym. Chem.* **1993**, *31*, 2493.
3. Li, J.; Zhao, L.; Guo, Sh. *J. Macromol. Sci. B* **2007**, *46*, 423.
4. Durmus, A.; Kasgoz, A.; Macosko, Chr. W. *Polymer* **2007** *48*, 4492.
5. Bhattacharya, A.; Mondal, S.; Bandyopadhyay, A. *Ind. Eng. Chem. Res.* **2013**, *52*, 14143.
6. Morlat, S.; Mailhot, B.; Gonzalez, D.; Gardette, J. -L. *Chem. Mater.* **2004**, *16*, 377.
7. Galgalia, G.; Agarwalb, S.; Lelea, A. *Polymer*, **2004**, *45*, 6059.
8. Lertwimolnun, W.; Vergnes, B. *Polymer*, **2005**, *46*, 3462.
9. Mihailova, M.; Krestev, M.; Aivazova, N.; Krestev, V.; Nedkov, E. *Radiat. Phys. Chem.*, **1999**, *56*, 581.
10. García-López, D.; Picazo, O.; Merino, J. C.; Pastor, J. M. *Eur. Polym. J.* **2003**, *39*, 945.
11. Gonzalez de los Santos, E. A.; Lozano Gonzalez, M. J.; Gonzalez, M. C. *J. Appl. Polym. Sci.* **1998**, *68*, 45.
12. Yazdani-Pedrama, M.; Vega, H.; Quijadab, R. *Polymer*, **2001**, *42*, 4751.
13. Lin, C. W. *J. Mater. Sci. Lett.* **1993**, *12*, 612.
14. Martínez, J. Ma. Ga.; Taranco, J.; Laguna, O.; Collar E. P. *Inter. Polym. Process.* **1994**, *9*, 246.
15. Zhang, M.; Colby, R. H.; Milner, S. T.; Chung, T. C. M. *Macromolecules*, **2013**, *46*, 4313.
16. Kim, H. S.; Lee, B. H.; Choi, S. W.; Kim, S.; Kim, H. J. *Compos. A Appl. Sci.* Manuf., **2007**, *38*, 1473.
17. Ko, T. M.; Ning, P. *Polym. Eng. Sci.* **2000**, *40*, 1589.
18. Lu, B.; Chung, T. C. *J. Polym. Sci. A Polym. Chem.* **2000**, *38*, 1337.
19. Pruthtikul, R.; Liewchirakorn, P. *Adv. Mater. Res.* **2010**, *93–94*,451.
20. Rzayev, Z. M. O. *Int. Rev.Chem. Eng.* **2011**, *3*, 153.
21. Mehrabzadeh, M.; Kamal, M. R.; Quintanar, G. *Iran. Polym. J.* **2009**, *18*, 833.
22. Simmons, A. Q.; Baker, W. E. *Polym. Eng. Sci.* **1989**, *29*, 1117.
23. Coutinho, F. M. B.; Ferfeira, M. I. *Eur. Polym. J.* **1994**, *30*, 911.
24. Ostenbrik, A. J.; Gaymans, R. J. *Polymer*, *33*, **1992**, 3086.
25. Ho, R. M.; Su, A. C. *Polymer*, **1993**, *34*, 3264.

26. Gaylord, N. G.; Metha, M. *J. Polym. Sci. Polym. Lett. Edu.* **1982**, *20*, 481.
27. Gaylord, N. G.; Mishra, M. K. *Polym. Sci. Polym. Lett. Edu.* **1983**, *21*, 23.
28. De Roover, B.; Sclavons, M.; Carlier, V.; Devaux, J.; Legras, R.; Momtaz, A. J. *J. Polym. Sci. A Polym. Chem.* **1995**, *33*, 829.
29. Gloor, P. E.; Tang, Y.; Kostanska, A. E.; Hamielec, A. E. *Polymer*, **1995**, *35*, 1012.
30. Heinen, W.; Rosenmoller, C. H.; de Groott, H. J. M.; Lugtenburg, J. *Macromolecules* **1996**, *29*, 1151.
31. Rusell, K. E.; Kelusky, E. C. *J. Polym. Sci. A Polym. Chem.* **1988**, *26*, 2273.
32. Moad, G. *Progr. Polym. Sci.* **1999**, *24*, 81.
33. Hogt, A. H.; Meijer, J.; Jelenic, J., Reactive Modifiers for Polymers, S. Al-Malaika, Blackie Academic Professional: London, **1997**; Chapter 1, p 32.
34. Dorscht, B. M.; Tzoganakis, C. *J. Appl. Polym. Sci.* **2003**, *87*, 1116.
35. Hogt, A. *ANTEC*, **1988**, *46*, 1478.
36. Bettini, H. P.; De Mello Lara, C.; Muñoz, P. A. R.; Ruvolo-Filho A. *J. Appl. Polym. Sci.* **2013**, *127*, 1001.
37. Sohn, C. H.; Shim, D. C.; Lee, J. W. *Macromol. Symp.* **2007**, *249-250*, 580.
38. Ajayan, P. M.; Schadler, L. S.; Braun, P. V., Nanocomposite Science and Technology; Wiley-VCH: New York, **2003**; Chapter 2, p 135.
39. Lopéz-Quintanilla, M. L.; Sanchez-Valdés, S.; Ramos-deValle, L. F.; Medellin-Rodriguez, F. J. *J. Appl. Polym. Sci.* **2006**, *100*, 4748.
40. Peng, B.; Wu, H.; Bao, W.; Guo, Sh.; Chen, Y.; Huang, H.; Lai; Sh. Y.; Jow, J. *Polym. Eng. Sci.* **2012**, *52*, 518.
41. Yaqin, Y.; Jun, Y. X. *J. Polym. Res.* **2011**, *18*, 2023.
42. Zhang, Y.; Chen, J.; Li, H. *Polymer* **2006**, *47*, 4750.
43. Xidas, P. I.; Triantafyllidis, K. S. *Eur. Polym. J.* **2010**, *46*, 404.
44. Vaia, R. A.; Giannelis, E. P. *Macromolecules* **1997**, *30*, 8000.
45. Costantino, A.; Pettarin, V.; Viana, J.; Pontesa, A.; Pouzada, A.; Frontinia, P. *Proc. Mater. Sci.* **2012**, *1*, 34.
46. Lapshin, S.; Isayev, A. I. *J. Vinyl Add. Technol.* **2006**, *12*, 78.
47. Swain, S. K.; Isayev, A. I. *Polymer* **2007**, *48*, 281.